# Generalised model for simulation of two- and three-phase cycle-dependent hysteresis in sandstones

Manuscript Accepted for Publication in Fuel Journal (Article reference: JFUE_JFUE-D-21-01827)

# A Generalised Model for Simulation of Two- and Three-phase Cycle-Dependent Hysteresis in Sandstones

**S. Aghabozorgi [1*], M. Sohrabi [1]**

[1] Centre for EOR and $CO_2$ Solutions, Heriot-Watt University, Edinburgh, UK

*Corresponding Author: For any correspondence regarding this manuscript please contact s.aghabozorgi_nafchi@hw.ac.uk

## Abstract

Many Enhanced Oil Recovery (EOR) processes involve injecting multiple slugs to improve the volumetric sweep efficiency in the reservoir, such as Water-Alternating-Gas (WAG), polymer flood, surfactant flood, and steam injection. Precise estimations of hysteresis phenomenon in relative permeability (kr) and capillary pressure (Pc) plays a crucial role in conducting accurate prognosis of oil production, reliable decision making, and feasibility assessment of EOR plans. Over the years, abundant high-quality experimental data revealed limitations of existing hysteresis models in the literature and highlighted the necessity of introducing a reliable hysteresis model.

This paper presents a new hysteresis model for accurate estimation of ultimate oil recovery and pressure drop in coreflood experiments. In contrast to the existing models, all required parameters are directly calculated from experimental data, eliminating the tuning procedure, and reducing the associated uncertainties. This study also includes a detailed discussion of estimating trapped gas saturation and application of Land's trapping model in cyclic systems, considering their importance in $CO_2$ sequestration and non-aqueous contaminant flow in soil. The presented model also benefits from a new procedure for estimating final saturations during a WAG experiment based on common observations of WAG experiments. A comprehensive set of cyclic two- and three-phase experiments performed on a homogenous sandstone over a wide range of injection scenarios, fluid, and rock properties were successfully used to validate the model. The detailed analysis and comparison of various cyclic experiments herein provide an excellent benchmark for future validation and development of hysteresis models.

**Keywords:**

Hysteresis in Relative Permeability, Multiphase Flow, Water Alternating Gas, Trapped Non-wetting Saturation, Land's Trapping Coefficient.

Manuscript Accepted for Publication in Fuel Journal (Article reference: JFUE_JFUE-D-21-01827)

# A Generalised Model for Simulation of Two- and Three-phase Cycle-Dependent Hysteresis in Sandstones


## Abstract

Many Enhanced Oil Recovery (EOR) processes involve injecting multiple slugs to improve the volumetric sweep efficiency in the reservoir, such as Water-Alternating-Gas (WAG), polymer flood, surfactant flood, and steam injection. Precise estimations of hysteresis phenomenon in relative permeability (kr) and capillary pressure (Pc) plays a crucial role in conducting accurate prognosis of oil production, reliable decision making, and feasibility assessment of EOR plans. Over the years, abundant high-quality experimental data revealed limitations of existing hysteresis models in the literature and highlighted the necessity of introducing a reliable hysteresis model.

This paper presents a new hysteresis model for accurate estimation of ultimate oil recovery and pressure drop in coreflood experiments. In contrast to the existing models, all required parameters are directly calculated from experimental data, eliminating the tuning procedure and reducing the associated uncertainties. This study also includes a detailed discussion of estimating trapped gas saturation and application of Land's trapping model in cyclic systems, considering their importance in $CO_2$ sequestration and non-aqueous contaminant flow in soil. The presented model also benefits from a new procedure for estimating final saturations during a WAG experiment based on common observations of WAG experiments. A comprehensive set of cyclic two- and three-phase experiments performed on a homogenous sandstone over a wide range of injection scenarios, fluid, and rock properties were successfully used to validate the model. The detailed analysis and comparison of various cyclic experiments herein provide an excellent benchmark for future validation and development of hysteresis models.


## Introduction

The hysteretic (history-dependent or irreversible) properties exist in various natural phenomena across physics, chemistry, engineering, and biology. Two essential properties of fluid flow are history-dependent: relative permeability and capillary pressure. Due to chemical heterogeneities or surface roughness in a porous medium, the advancing contact angle is larger than the receding contact angle, called the contact angle hysteresis. As the wetting phase invades the porous medium during an imbibition process, a fraction of the non-wetting phase becomes disconnected and trapped. The overall impact of these two phenomena is that the

relative permeability and capillary pressure data are not identical for drainage and imbibition processes [1, 2].

The common perception of hysteresis in relative permeability is mainly associated with a multi-phase system in which the saturation path is reversed from primary drainage to imbibition or vice versa (usually referred to as “Directional Hysteresis” or “Conventional Hysteresis”). However, another form of it is often observed in processes involving cyclic injection plans such as WAG experiments, cyclic steam injections, non-aqueous contamination flow in porous media, or cyclic injection scenarios to enhance $CO_2$ trapping in underground reservoirs [3-5]. The terms “cyclic hysteresis” and “cycle-dependent relative permeability” are used interchangeably in the literature to emphasize the effects of cyclic injection (Figure 1).

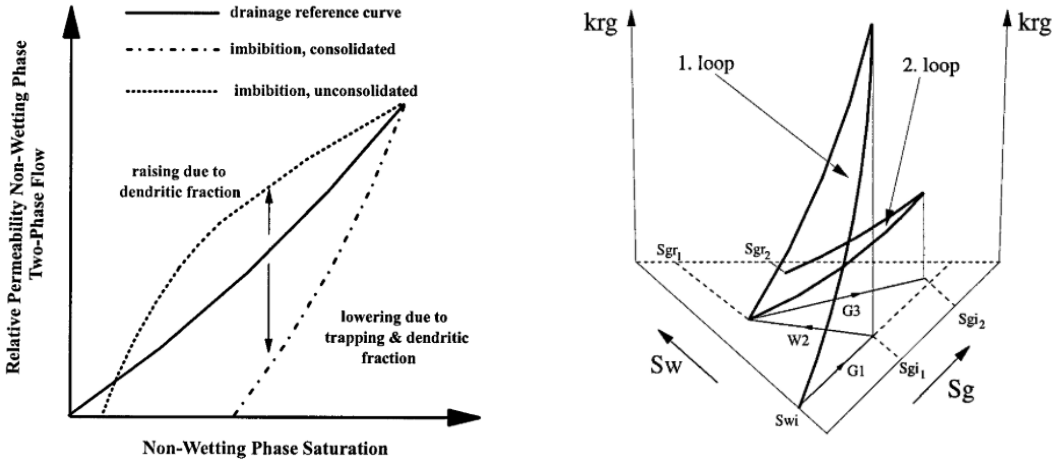


(a) (b)

Figure 1: Observed hysteresis loops in (a) two-phase system undergoing flow reversal from drainage to imbibition, (b) three-phase system undergoing cyclic injection [6].

Hysteresis effects in kr data were first observed and reported for a two-phase system undergoing flow reversal from primary drainage to imbibition [7]. It was also stated that the imbibition relative permeability curve is reversible if the imbibition process is followed by another drainage cycle. This reversibility assumption was initially proposed based on the observed behaviour in water-wet samples. However, Land, Carlson, and Killough adopted the same postulation when developing their hysteresis models, which are currently used for all wettability conditions [8-10]. The reported results of two-phase cyclic experiments performed in mixed-wet samples prove that this assumption is not valid in these systems, and inattentive use of hysteresis models in simulations can cause significant errors [11].

A scrutiny review of the literature reveals alarming issues associated with the existing hysteresis model that seem to be overlooked. First and foremost, some of these models were not validated using a comprehensive set of experimental data [10]. The other ones have only reported the obtained relative permeability curves, raising concerns regarding the quality of the match with the observed pressure drop curve [4, 12]. Second, using these models involves a tedious history matching or tuning process, increasing the uncertainty in the results [13, 14]. Lastly, the existing models cannot be used for both two- and three-phase systems. Ideally the formulations of a three-phase hysteresis model should apply to two-phase systems by setting appropriate variables equal to zero.

The most comprehensive three-phase hysteresis model implemented in commercial software such as Eclipse, Intersect, and CMG is the one published by Larsen and Skauge [6]. Even though this nicely structured model follows a logical procedure for estimation of the hysteresis phenomenon, there are some issues regarding the formulations and assumptions of each step:

1. *Calculation of three-phase relative permeability:* Multiple formulations exist in the literature to estimate three-phase oil kr data from two-phase kr data. Such models are conventionally referred to as 3P-kr models in the literature. Two-phase kr data, krow and krog, are measured respectively in an oil/water system and a gas/oil system in the presence of connate water. The hysteresis model introduced by Larsen and Skauge uses Stone I formulation for deriving the three-phase oil relative data [15]; however, it can be coupled with other models such as saturation-weighted interpolation or Baker's when using commercial software[16]. A recent study shows that these models cannot reproduce the gradual oil production observed in WAG experiments[17]. Larsen and Skuage assume negligible hysteresis in three-phase oil kr data.
2. *Estimation of saturations at the end of each cycle:* Accurate estimation of trapped gas saturation is vital for calculating hysteresis in gas relative permeability and determination of residual oil saturation at the end of each cycle. The aforementioned model uses a modified version of Land's initial-residual relationship to calculate dynamic trapped saturation in each cycle; then exploits the formulation developed by Holmgren and Morse to obtain the residual oil saturation[18]. Multiple studies have revealed that a single value of Land's constant cannot provide a good match for the entire experiment. Even though trapping coefficient is regarded as an intrinsic physical

parameter of the rock, the user should vary it in each cycle to obtain a reasonable match [12, 19-21].

3. *Formulations for estimation of hysteresis in water and gas relative permeability:* This model introduces multiple formulations for calculating water relative permeability applicable to different possible saturation paths. These formulations are only valid if the first three-phase water injection cycle is started at the maximum non-wetting saturation, which is not the case in many WAG experiments. The hysteresis in gas relative permeability is governed by a reduction factor(α) which needs to be determined through the history matching process. In some cases, changing this parameter can result in convergence issues[22, 23].

The performance of the WAG hysteresis model mentioned above in the prediction of experimental data, especially pressure drop and trapped gas saturation, has been discussed in great detail in another due publication [22].

Currently, there are two approaches for the simulation of WAG experiments. The first one is to use Larsen and Skauge model and then tune its parameters (Land's coefficient, Holmgren and Morse constant, and gas reduction factor) until a good match is obtained [13, 14]. Another approach is to history match each cycle individually to find the three-phase relative permeability values for oil, water, and gas directly as a multivariant function of the other two saturations [24]. The latter approach has been facilitated by using 2D tables in ECLIPSE commercial software and is implemented the in-house software called 3RPSim for history matching of unsteady-state three-phase experiments.

The new hysteresis model presented in this paper follows the same three-step procedure discussed above. However, the formulations in each step were developed so as most of the parameters could be attained directly from the experimental data to reduce the hassle of parameter tunning or history matching procedure. In its current form, only one parameter of this model needs to be obtained through the tuning process. All other parameters (for estimation of final saturations, gas, and water relative permeability) are calculated directly from the experimental data.

Various cyclic two- and three-phase experiments performed in 'Centre for Enhanced Oil Recovery and CO2 Solutions' at Heriot-Watt University have resulted in an extensive dataset that can be used to validate hysteresis models. These experiments were performed with different injection scenarios, i.e., starting with imbibition or drainage [25, 26], on water-wet,

mixed-wet, and oil-wet samples [27-30], at different IFT values[31, 32], and using different homogeneous and heterogeneous rock types [33]. These researches have also studied oil and gas trapping in cyclic two- and three-phase experiments [20]. These experimental data were used in this study for validation and comparison purposes. Consistent abbreviations are used throughout this paper for referencing the experiments as adopted by Fatemi et al.: "MW" and "WW" stand for mixed-wet and water-wet conditions, "ImM" and "NM" represent immiscible and near-miscible conditions, and imbibition and drainage processes are widely replaced by "I" and "D" respectively[34]. The fluids were pre-equilibrated to minimize the mass transfer between fluids during the experiments. A detailed discussion of the experimental setup and preparation procedure for all experiments can be found in the literature[34]. The properties of rock and fluid used in the experiments are briefly mentioned in Table 1 to Table 3.

Table 1: The properties of the Clashach Sandstone used in the experiments.

| Sample | Length (cm) | Diameter (cm) | Permeability (md) | Porosity (frac.) |
|---|---|---|---|---|
| Clachach Sandstone | 60.5 | 5.082 | 65 | 0.18 |
| Indiana Limestone | 59.9 | 4.96 | 45 | 0.15 |

Table 2:The properties of synthetic brine used in the experiments.

| Salinity (mg/L) | Density @ 38ºC (g/L) | Viscosity @ 38ºC (cp) |
|---|---|---|
| 1000 | 992.96 | 0.68 |

Table 3: Properties for hydrocarbon mixture at 100°F.

| Pressure (psi) | $\rho_g$ ($kg/m^3$) | $\rho_L$ ($kg/m^3$) | $\mu_g$ (mPa.s) | $\mu_L$ (mPa.s) | IFT (mN/m) |
|---|---|---|---|---|---|
| 1840 | 211.4 | 317.4 | 0.0249 | 0.0405 | 0.04 |
| 1200 | 86.68 | 466.06 | 0.0141 | 0.0793 | 2.7 |

The model's performance was successfully evaluated using the experimental data published by Fatemi et al., and the results are presented in this paper. In contrast to the available hysteresis models in the literature, by setting the saturation of one phase equal to zero, the formulations were successfully used for simulating cyclic two-phase experiments performed on sandstone rock.

## Model Description

As mentioned in the introduction, the new hysteresis model discussed in this paper follows the same three-step structure adopted by Larsen and Skauge to (a) estimate three-phase oil relative permeability, (b) trapped gas saturation, and fluid saturation at the end of each cycle, and (c) reduction in water and gas kr data. However, the formulations used in each step are different, which are discussed in this section in detail. By using the term "generalised", we emphasise on the application of the model for simulating both two- and three-phase systems.

### *1. Modification of 3P-Kr models*

3P-kr models available in the literature are primarily developed based on steady-state three-phase flow measurements where the oil, water, and gas phases are co-injected. Conversely, WAG experiments usually involve the injection of one phase (either gas or water) into a porous medium where the oil phase is disconnected or partially connected. As expected, the relative permeability of the oil phase is higher in steady-state experiments and using 3P-kr models results in an overestimation of kr data in WAG experiments.

This discontinuity of the oil phase and reduction in relative permeability was reported in the literature for steady-state experiments performed at very low oil saturation. Stone's exponent model was proposed to address this issue and increase the accuracy of the results in such conditions [35], but unfortunately, this model cannot reproduce the gradual oil production trend observed in WAG experiments (Figure 2).

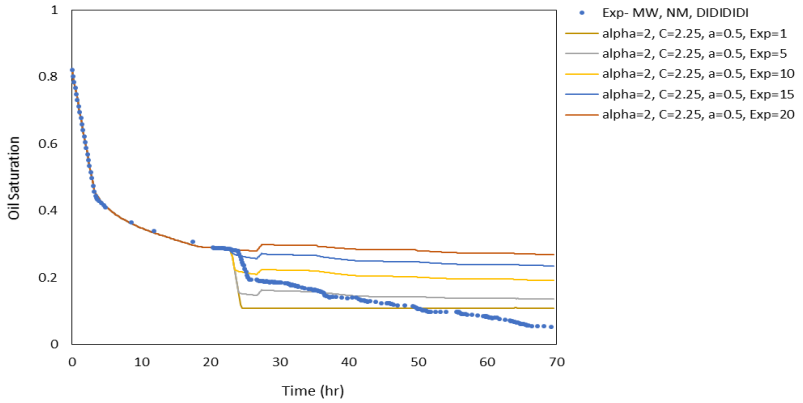


(a)

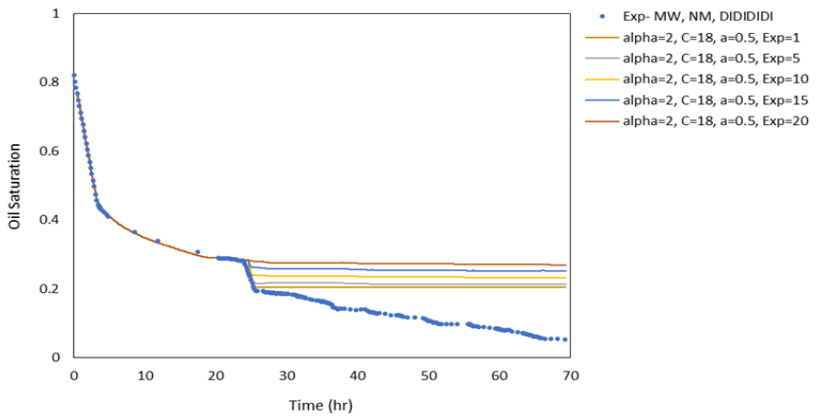


(b)

Figure 2: Stone's Exponent model's performance in predicting oil saturation (alpha, C, and a are tuning parameters for Larsen and Skauge hysteresis model) [17].

In this study, Stone's model was modified by introducing a reduction factor ($\beta_o$) to overcome this obstacle and improve the estimation of oil production in low oil saturation range [17]:

For $S_o > S_{orw}$ (Stone I):

$$k_{ro} = k_{rocw}.\, SS_o.F_w.F_g\,, \qquad S_{om} = 0 \tag{1}$$

For $S_o < S_{orw}$ (Modified Stone I):

$$k_{ro} = \beta_o\,.\, k_{rocw}.\, SS_o.F_w.F_g\,, \qquad S_{om} = 0 \tag{2}$$

In which $SS_o$, $F_w$ and $F_g$ are calculated according to Stone's model and $k_{rocw}$ is the oil relative permeability measured at connate water saturation. The formulation is identical to Stone's first model when the reduction factor ($\beta_o$) is equal to unity. This reduction factor is obtained by tuning; however, an improved match for early cycles is adequate as the rest of the cycles will be matched automatically later when appropriate formulations are used to estimate hysteresis in water and gas kr data (Figure 3).

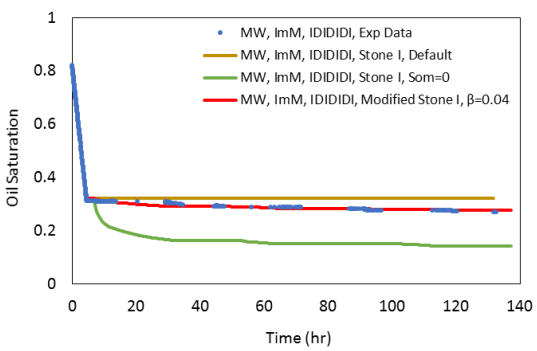


(a)

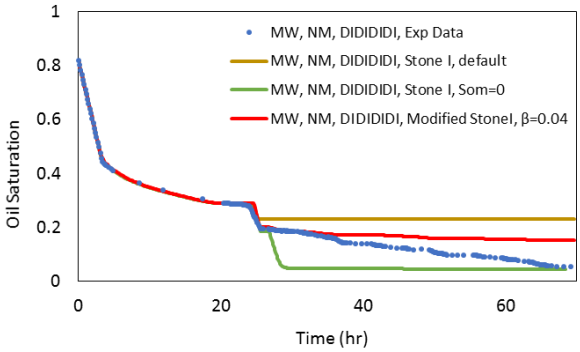


(b)

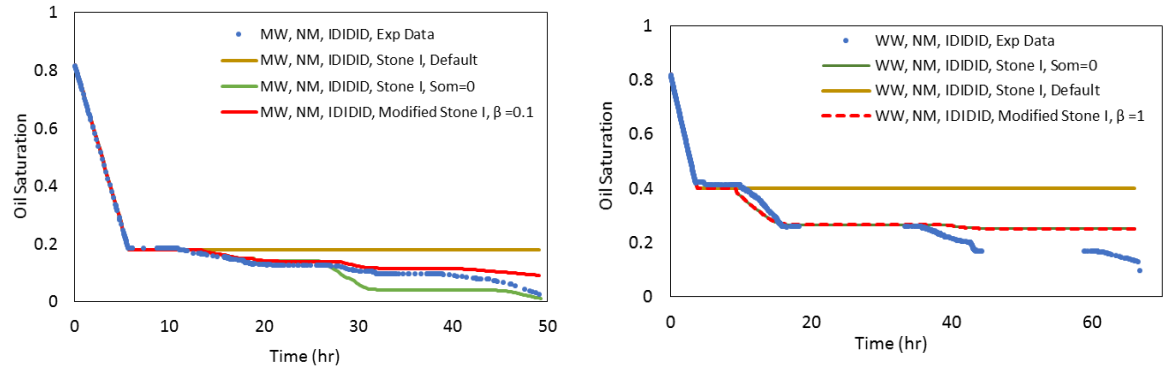


(c) (d)

Figure 3: The performance of Stone I and modified Stone model in prediction of oil saturation profile [17].

## 2. *A New Approach for Estimation of $S_{gt}$ and $S_{om}$*

In the model proposed by Larsen and Skauge, the formulations used to estimate the reduction in gas and water kr data are a function of trapped gas saturation ($S_{gt}$). The estimation of residual oil saturation ($S_{om}$) also depends on $S_{gt}$. Therefore, any error in the calculation of trapped gas saturation enters multiple formulations and grows as the simulation moves forward. Conventionally, Land's initial-residual relationship is used for this purpose, though the use of this formulation for the estimation of dynamic trapped saturation is questionable[36].

In addition, this relationship is based on the results of two-phase oil/gas experiments at irreducible water saturation, and its application in three-phase systems with mobile water saturation needs to be verified experimentally. Another nuance to consider is that for obtaining one point of an initial-residual graph, the experiment is started at a specific initial saturation. Then the injection rate of displacing fluid is increased until no more non-wetting phase is produced, and the system has reached "residual" saturation. The exact process is repeated at various initial saturations to obtain multiple points and calculate Land trapping coefficient by fitting the curve. In many WAG experiments and reservoir blocks, saturations at the end of each cycle do not necessarily reach "residual" values, and this signifies another drawback of using Land's formulation for three-phase WAG experiments. The WAG experiments presented in this paper are performed at a constant injection rate, and the injection rate was not increased in each cycle to ensure reaching the residual saturation; consequently, the final gas saturations do not obey Land's relationship. Figure 4 clearly shows that trapping coefficient should be changed throughout the simulation for a precise estimation of trapped gas saturation.

Throughout this manuscript, saturations at the end of each cycle are called “final” saturation to highlight this critical difference.

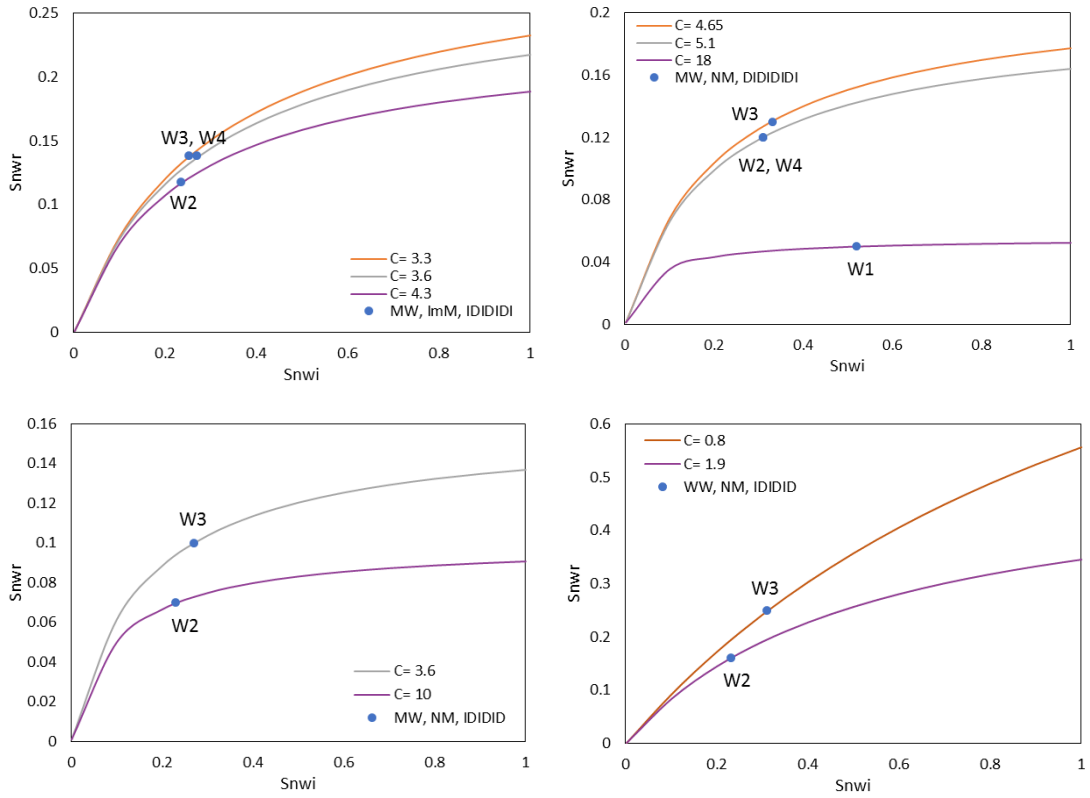


Figure 4: Initial-final gas saturations at the end of imbibition cycles for the WAG experiments compared with the Land’s initial-residual curves.

Figure 5 shows the trend of final saturations measured at the end of each injection cycle for different WAG experiments performed on a sandstone sample. The oil and water saturation profiles show that the reduction in oil saturation is gradual and monotonic, while the water saturation fluctuates in a specific range). In this study, the formulations for calculating final saturations are based on these two trends rather than Land’s initial-residual relationship.

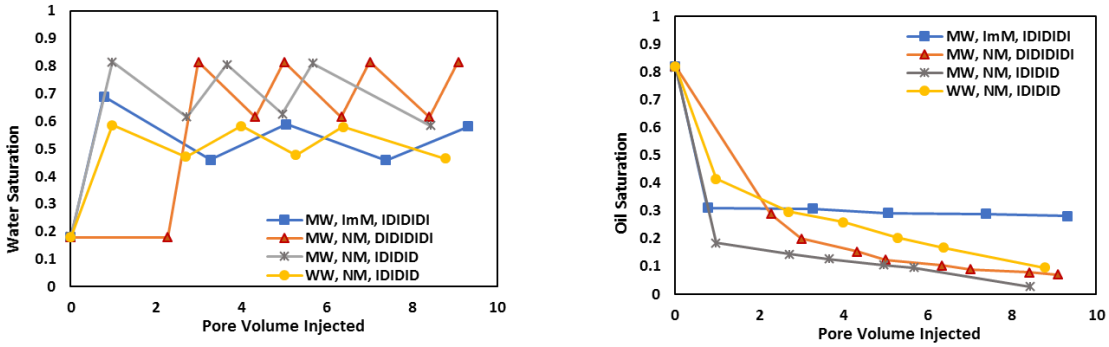


Figure 5: The observed trend in water and oil saturation, WAG experiments performed on the sandstone sample.

To quantify the monotonic decline in oil saturation, a new parameter called "relative difference" is defined for estimating the reduction in oil saturation in each cycle:

$$\delta_o = \left(\frac{S_{of}^{n} - S_{of}^{n-1}}{S_{of}^{n}}\right) \quad (3)$$

In which $S_{of}^{n}$ is the final oil saturation measured at the end of n$^{th}$ injection cycle. The relative difference for oil saturation ($\delta_o$) is calculated for all cycles of the WAG experiment (except the first two-phase cycles). An arithmetic average is then obtained ($\delta_{o,ave}$) since the injected pore volume might vary for different injection cycles. The accuracy of the model increases as the number of injection cycles increases. The final value of oil saturation at the end of each injection cycle is:

$$S_{of} = (1 - \delta_{o,\ ave}).\ S_{of}^{n-1} \quad (4)$$

It is also assumed that the final water saturations change in a specific saturation range (between the initial and final water saturations of the second waterflood). This assumption is valid in the systems where the reduction in water saturation is negligible (or assumed to be negligible):

$$S_{wf} = \begin{cases} S_{wi}^{W2} & S_w\ at\ Begining\ of\ the\ Imbibition\ Cycle \\ S_{wf}^{W2} & S_w\ at\ the\ End\ of\ the\ Imbition\ Cycle \end{cases} \quad (5)$$

In cases where the reduction in water saturation is not negligible (e.g., two-phase systems), the relative difference for water saturation ($\delta_w$) in each cycle is calculated as follows:

$$\delta_w = \left(\frac{S_{wf}^{n} - S_{wf}^{n-1}}{S_{wf}^{n}}\right) \quad (6)$$

Usually, the injected pore volume is not constant during different cycles; so, an average reduction factor is used in the simulations ($\delta_{w,ave}$). The final value of water saturation at the end of each injection cycle is then updated as:

$$S_{wf} = (1 - \delta_{w,\ ave}).\ S_{wf}^{n-1} \quad (7)$$

the value of gas saturation is then calculated as:

$$S_{gf} = 1 - S_{of} - S_{wf} \quad (8)$$

When using this method, the user is suggested to first calculate the relative permeabilities assuming negligible changes in water saturation. If the results were not satisfactory, then the

reduction in water saturation should be considered in the simulation. Even though this new method calculates the gas saturation indirectly, it can capture the gradual change in the trapped gas saturations with great accuracy. Furthermore, the estimated average reduction factors are calculated directly from the experimental data, eliminating the hassle of a trial-and-error tuning process.

Table 4 presents the average relative differences in water and oil saturations calculated for each WAG experiment. The average changes in water saturation for three experiments (exp 1, 3, and 4) were negligible compared to the average changes in oil saturation at the end of cycles. The changes in the water saturation were greater in the second experiment compared to the other tests, but the saturation profiles were successfully reproduced, assuming negligible changes in water saturation. For simulation of two-phase experiments, the average relative difference was calculated for the water phase, and the saturation of non-wetting phase was determined accordingly.

Table 4: Comparison of the average relative difference in oil and water saturations.

| Experiment | Decrease in $S_o$ | Changes in $S_w$ |
|---|---|---|
| (1) MW, IDIDIDI, IM | 4 % | < 1 % |
| (2) MW, DIDIDI, NM | 23.5 % | 9 % |
| (3) MW, IDIDID, NM | 15 % | 3 % |
| (4) WW, IDIDID, NM | 20 % | < 1 % |

### *3. Estimation of Reduction in Water and Gas Relative Permeability*

In this new model, the scanning curves of water relative permeability are estimated for imbibition cycles and then assumed to be reversible in drainage cycles. For imbibition cycles, the water kr data is calculated as follows:

$$K_{rw}^{n} = \beta_w . K_{rw}^{n-1} \quad (9)$$

in which $\beta_w$ is the reduction factor for water kr data and is calculated using the stabilized pressure drop measured at the end of imbibition cycles as follows:

$$\beta_w = \Delta P\,(S_{wf}^{n-2}) / \Delta P\,(S_{wf}^{n}) \quad (10)$$

in which $S_{wf}$ is the final water saturation measured at the end of the injection cycle, and $n$ represents the number of injection cycles. The gas relative permeability curves for drainage cycles can be estimated using the following equation:

$$K_{rg}^{n} = \beta_g . K_{rg}^{n-1} \quad (11)$$

where $\beta_g$ is the reduction factor for gas kr data and calculated again using the stabilized pressure measured at the end of the drainage cycles:

$$\beta_g = \Delta P\ (S_{gf}^{n-2}) / \Delta P\ (S_{gf}^{n}) \quad (12)$$

For the imbibition cycles, another formulation is proposed to maintain the continuity in the gas kr data:

$$K_{rg}^{n} = (\frac{S_g - S_{gi}^{n}}{S_{gf}^{n} - S_{gi}^{n}}).\ K_{rg}^{n-1} \quad (13)$$

In this equation $S_{gi}$ and $S_{gf}$ are the initial and final gas saturations for each injection cycle, and n represents the number of injection cycles. These initial and final saturations are the values calculated according to the formulations discussed in the previous section.

## Results and Discussion

### 1. Simulation of WAG experiments

Figure 6 to Figure 9 shows the model's performance for matching the oil saturation profiles and pressure drop curves of four WAG experiments. As observed, even though the experiments are performed in various conditions, the gradual oil production has been simulated with great accuracy. The obtained results are remarkable considering the fact that the model's parameters were calculated directly from the experimental data, and no tuning procedure was followed. The pressure drop curve is slightly mismatched, possibly due to hysteresis in capillary pressure, which is not considered in this study.

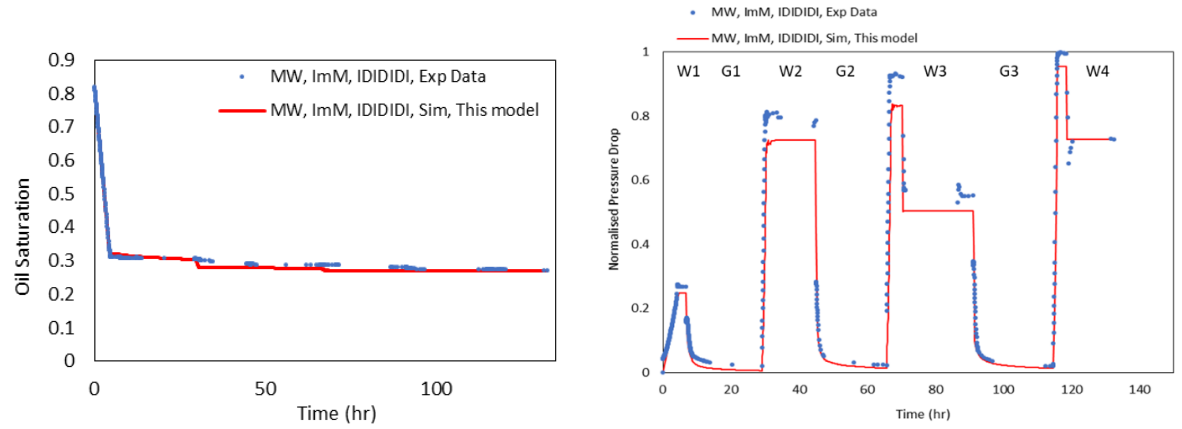


(a) (b)

Figure 6: Comparison of predicted values with measured data for WAG experiment No.1 (MW, ImM, IDIDIDI).

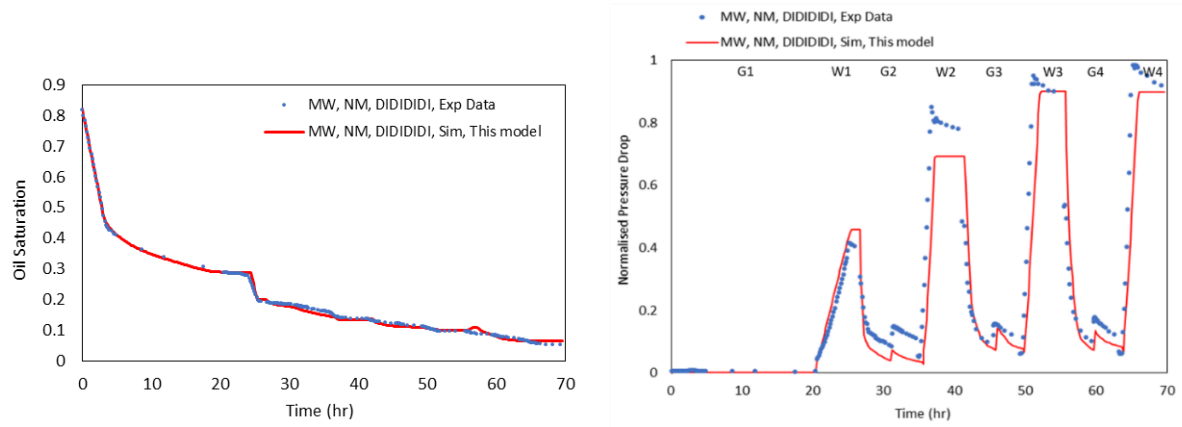


(a) (b)

Figure 7: Comparison of predicted values with measured data for WAG experiment No.2 (MW, NM, DIDIDIDI).

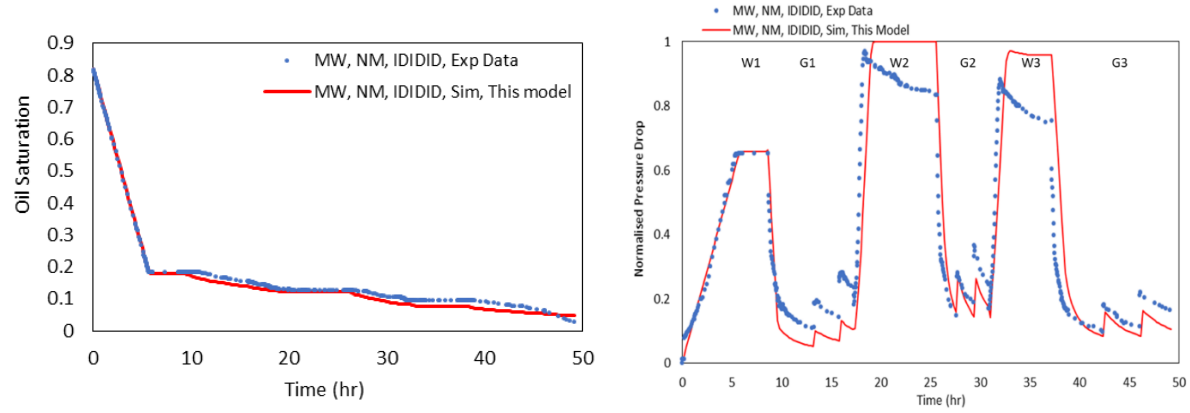


(a) (b)

Figure 8: Comparison of predicted values with measured data for WAG experiment No.3 (MW, NM, IDIDID).

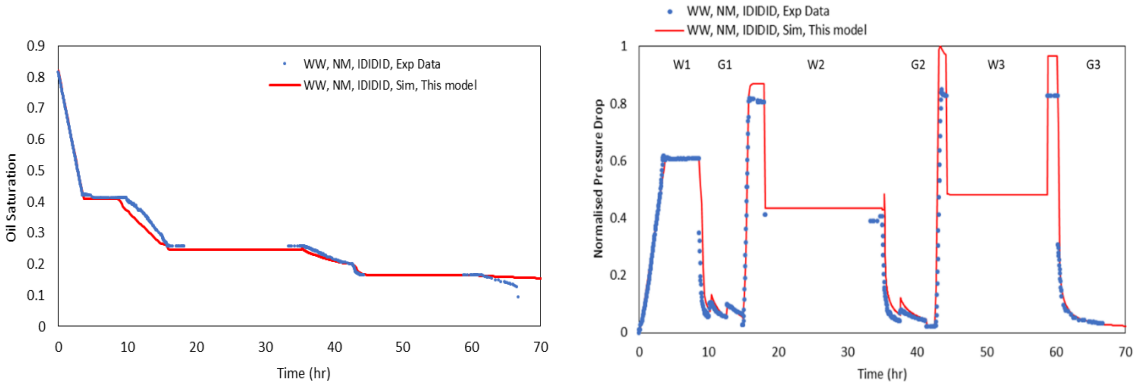


(a) (b)

Figure 9: Comparison of predicted values with measured data for WAG experiment No.4 (MW, NM, DIDID).

The absolute and relative errors with respect to the experimental data were calculated and reported to evaluate the accuracy of estimated gas and water saturations. In this study, relative errors were calculated for total production, and absolute errors were reported for predicted saturations (as the saturations are already relative values with respect to the pore volumes):

$$\text{Relative Error in Production} = \frac{Q_{sim} - Q_{exp}}{Q_{exp}} * 100 \quad (23)$$

$$\text{Absolute Error in Saturations} = S_{sim} - S_{exp} \quad (24)$$

Figure 10 to Figure 13 show the error in prediction of final saturations for four experiments. The positive values of absolute error indicate an overestimation, while negative values indicate an underestimation of fluid saturations (graph b). The summation of errors in estimating oil, water and gas saturation is equal to zero at the end of each cycle. A closer look at the relative errors in fluid production reveals that the calculated error is below 4% in all cycles of WAG experiments except in two cycles, an indication of significant improvement in the estimation of fluid production in WAG experiments. Even though trapped gas saturation is not calculated directly, the error in the estimation of final gas saturations is less than 3% in most of the cycles.

Looking at Figure 11, the error in the estimation of fluid production is higher for first water and second gas injection cycles of the experiment performed on mixed-wet rock, at near miscible condition, starting with gas (experiment No.2). Despite the significant error in these two cycles, the error in the estimation of total fluid production (calculated at W4) is less than

2% which is very promising. This signifies the importance of averaging technique when calculating the reduction factor in water and gas saturation.

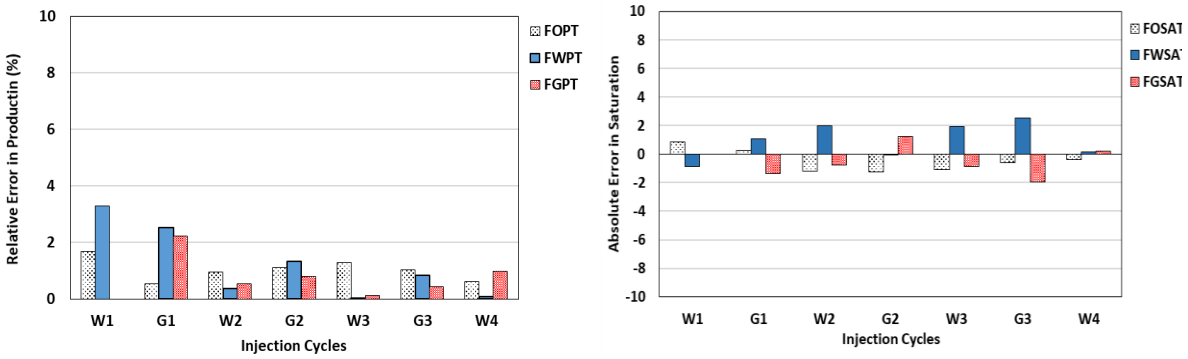


(a) (b)

Figure 10: (a) Relative error in fluid production and (b) Absolute error in saturation; WAG experiment No.1 (MW, ImM, IDIDIDI).

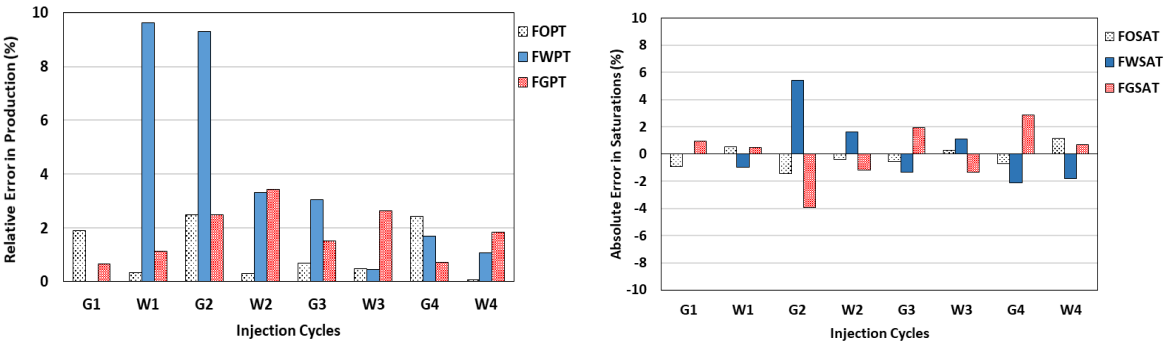


(a) (b)

Figure 11: (a) Relative error in fluid production and (b) Absolute error in saturation; WAG experiment No.2 (MW, NM, DIDIDIDI).

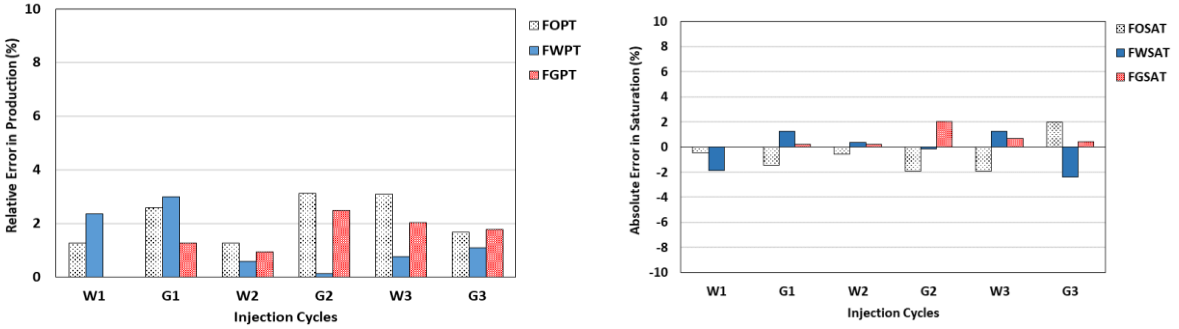


(a) (b)

Figure 12: (a) Relative error in fluid production and (b) Absolute error in saturation; WAG experiment No.3 (MW, NM, IDIDID).

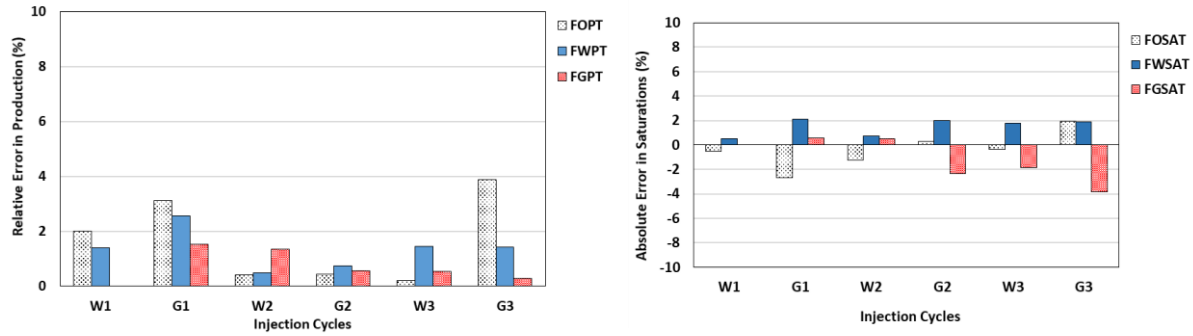


(a) (b)

Figure 13: (a) Relative error in fluid production and (b) Absolute error in saturation; WAG experiment No.4 (WW, NM, IDIDID).

Figure 14 compares the errors in estimated pressure drop values at the end of each cycle for the four WAG experiments discussed previously. The results show that the error in the estimation of pressure drop at the end of gas injection cycles is more significant than that for water injection cycles. One reason could be that the capillary pressure has been considered constant in these simulations (i.e., the hysteresis in capillary pressure was considered negligible). In gas injection cycles, the order of capillary pressure is comparable to the viscous force, and any changes in its value can significantly affect the results. This mismatch is expected to decrease if appropriate equations are introduced in the simulation for estimating hysteresis in capillary pressure. In the reported experiments, the injected slug size and core length are large enough to ensure minimising the capillary end effect. However, this is not the case in Short Slug Water Alternative Gas (SSWAG) experiments, so using the presented model for simulation of such experiments needs to be evaluated.

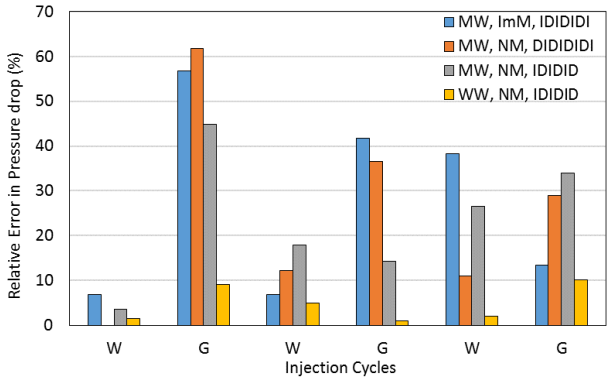


Figure 14: Comparison of error in the estimation of pressure drop in four different WAG experiments.

## 2. Cyclic Two-Phase Experiments

Currently, observed hysteresis phenomena in two-phase systems are widely simulated using Carlson's and Killough's models implemented in Eclipse software [9, 10]. As mentioned before, these models were developed based on the experimental data obtained from water-wet samples and have adopted the negligible cyclic hysteresis assumption suggested by Geffen et al.. In this part of the study, three set of simulation results are presented to compare the performance of existing models and the developed model with the experimental data. The hysteresis in the capillary pressure is not considered in these simulations to investigate the impact of hysteresis in kr data on final results exclusively.

The first set of simulations is performed to test the validity of negligible cyclic hysteresis assumption in two-phase mixed-wet systems. The primary drainage and the following imibition cycle are history matched to obtain the kr data. The history-matched imbibition kr data is used for simulation of subsequent cycles using Eclipse software. Figure 15 and Figure 16 show that this assumption does not capture the increased pressure drop trend observed in the experimental data. In addition, the changes in trapped non-wetting saturation during imbibition cycles cannot be predicted accurately.

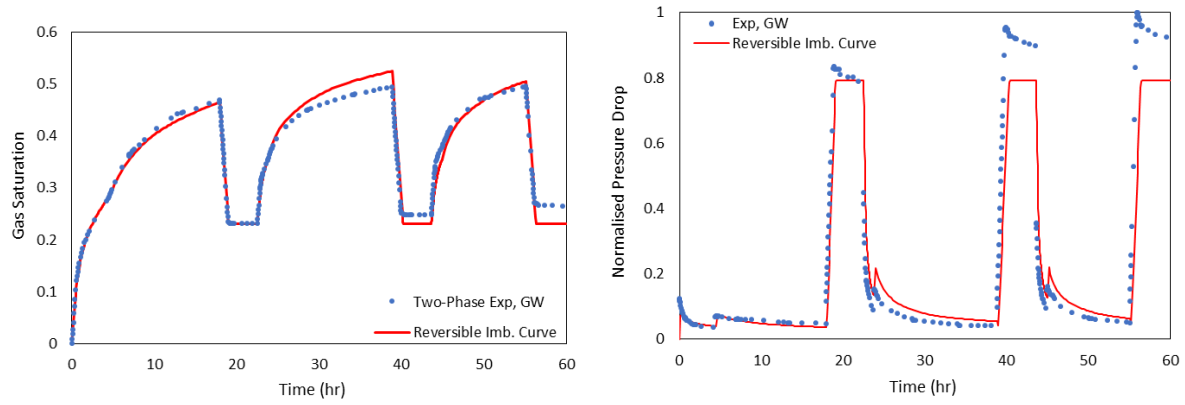


(a) (b)

Figure 15: The simulation results obtained assuming reversible imbibition kr curve compared with experimental data (cyclic gas/water experiment started with gas injection).

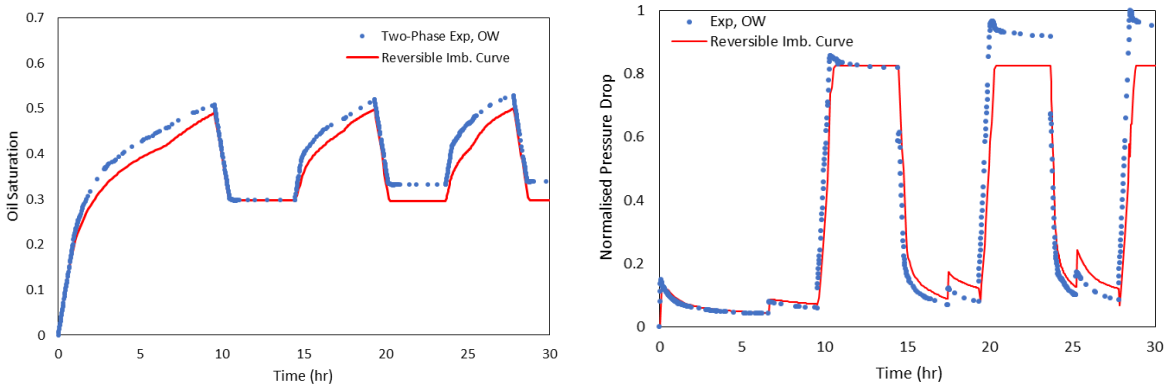


(a) (b)

Figure 16: The simulation results obtained assuming reversible imbibition kr curve compared with experimental data (cyclic oil/water experiment started with oil injection).

The second set of simulations are performed by activating Carlson's and Killough's model implemented in Eclipse software. Activation of this option requires two saturation tables, one for drainage and one for imbibition kr data. Table 5 shows five options available in Eclipse software for the estimation of the wetting and non-wetting kr data.

Table 5: The options available in Eclipse Software for simulation of the hysteresis phenomenon.

| EHYSTR Keyword | Model used for Non-Wetting phase | Table used for Wetting Phase |
|---|---|---|
| 0 | Carlson's model | drainage (SATNUM) |
| 1 | Carlson's model | imbibition (IMBNUM) |
| 2 | Killough's model | drainage (SATNUM) |
| 3 | Killough's model | imbibition (IMBNUM) |
| 4 | Killough's model | Killough's model |

A comparison of experimental data with the obtained results are presented in Figure 17 and Figure 18 for both gas-water and oil-water experiments. It can be observed that the value of trapped non-wetting saturation at the end of each imbibition cycle is not simulated accurately. In cases that the error in the estimation of pressure drop is low, the error in estimation of saturation profile is high and vice versa.

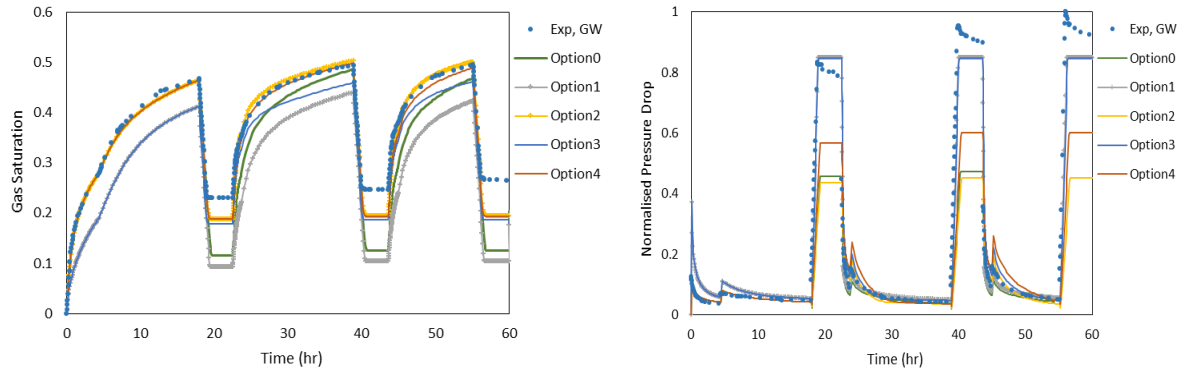


(a) (b)

Figure 17: The simulation results obtained by activating the implemented model compared with experimental data (gas-water experiment).

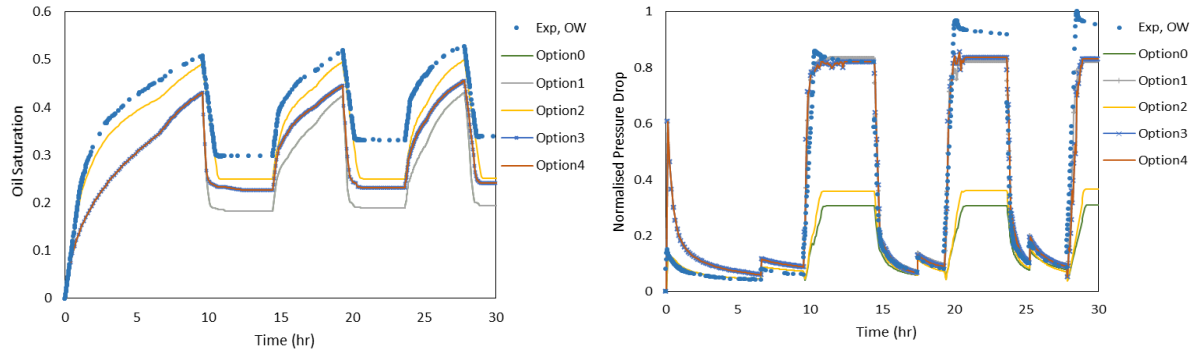


(a) (b)

Figure 18: The simulation results obtained by activating the implemented model compared with experimental data (oil-water experiment).

The third set of simulations presented is performed using the developed hysteresis model in this study and by setting the parameters of one phase equal to zero. For the weakly water-wet and oil-wet samples, the formulations for estimation of wetting and non-wetting saturation have the following form:

$$(\delta_w) = \left(\frac{S_{wf}^{n} - S_{wf}^{n-1}}{S_{wf}^{n}}\right) \tag{14}$$

$$S_{wf} = \delta_{w,\,ave}.\, S_{wf}^{n-1} \tag{15}$$

$$S_{nw-f} = 1 - S_{wf} \tag{16}$$

Looking at the results (Figure 19 and Figure 20), one can quickly notice the improvement in simulation results. Unlike the results obtained using the available hysteresis models for two-phase systems, the increase in trapped non-wetting saturation is calculated successfully. The

reduction in water and oil kr data was minimal, but the impact of this change on pressure-drop values was not negligible. Similar to the three-phase experiments, it is likely that the observed mismatch during second and third gas injection cycles is due to the hysteresis in capillary pressure.

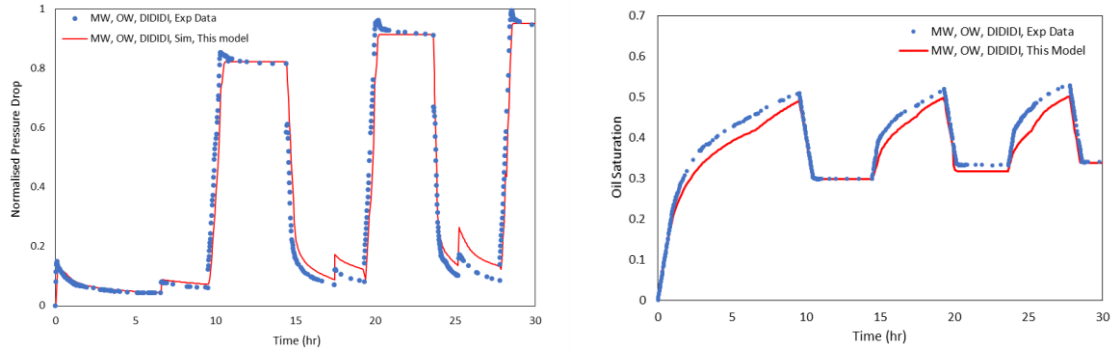


(a) (b)

Figure 19: The simulation results obtained using the presented model compared with experimental data (oil-water experiment).

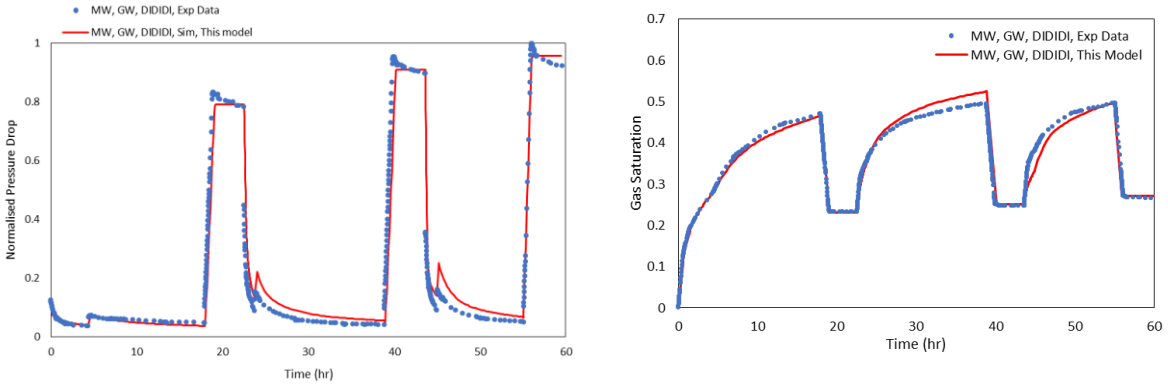


(a) (b)

Figure 20: The simulation results obtained using the presented model compared with experimental data (gas-water experiment).

## 3. Common Observations of Cyclic experiments

One of the important questions asked when designing a WAG experiment is the number of injection cycles that need to be performed to obtain adequate data for proper simulation of hysteresis phenomena. The effect of cyclic hysteresis on flow behaviour may not be fully observed in a short WAG experiment; on the other hand, performing a long experiment is both expensive and time-consuming.

Table 6 shows the values obtained for various parameters of the new WAG hysteresis model described in this paper. The results show that the values of the reduction factor in gas and water kr data increase and reach values close to unity, meaning that after several cycles, the hysteresis in gas and water kr data is negligible in the system. In other words, after several cycles, distinguished flow paths are established for each phase in the system, and no more gas can be trapped. Therefore, the WAG experiments need to be continued until no further changes are observed in the pressure drop or fluid saturations. For a homogeneous sandstone similar to the one used in this study, the system has reached this stage after eight cycles of injection (four cycles of water injection and four cycles of gas injection).

Table 6: The values of various parameters obtained in this paper for simulation of WAG experiments.

| **Experiment** | $\delta_o$ | $\beta_o$ | $\beta_w$ | $\beta_g$ |
|---|---|---|---|---|
| (1) MW, IDIDIDI, IM | 0.023 | 0.04 | 0.375 - 0.88 - 0.94 | 0.5 - 1 |
| (2) MW, DIDIDI, NM | 0.19 | 0.04 | 0.5 - 0.868 - 0.96 | 0.5 - 0.85 |
| (3) MW, IDIDID, NM | 0.26 | 0.1 | 0.68 - 1 | 0.75 - 1 |
| (4) WW, IDIDID, NM | 0.25 | 1 | Matched with $\beta_w$=1 | 0.41 – 0.54 |
| (5) MW, IDIDI, GW | - | - | 0.87, 0.95 | $\beta_g$ =1 |
| (6) MW, IDIDI, OW | - | - | 0.9, 0.96 | $\beta_o$ =0.9 |

The oil production in immiscible WAG experiments is almost ceased after the first two cycles, while near-miscible experiments show a gradual oil production. The hysteresis model presented in this paper reproduced the oil production trend in both cases successfully, and there is no need to differentiate the hysteresis behaviour according to the IFT values. To summarise, the common features observed in cyclic two- and three-phase experiments performed on the homogeneous sandstone sample at various conditions can be categorised as follows:

1) *Monotonic decrease in oil saturation:* the oil saturation decreases monotonically in all experiments (observed only in three-phase experiments),

2) *Systematic changes in water saturation:* Water saturations change between a maximum and a minimum value (observed only in three-phase experiments),

3) *Increase in the pressure drop*: An increase in the trapped saturations results in an increase in observed pressure drops during subsequent cycles of gas or water injection,

4) *Significant difference in pressure-drop values measured during drainage and imbibition cycles*: The pressure drop in drainage cycles is significantly lower than imbibition cycles,

5) *Reduction in the observed hysteresis during last cycles:* there are almost no changes in the pressure drop and trapped gas saturation as the experiment continues towards the last cycles.

The increase in pressure drop is observed in almost all cycles of two- and three-phase experiments, except the last cycle of one experiment No.3 (Figure 8) that can be attributed to experimental error.

**Implementation of the Model in Reservoir-Scale Simulations**

For simulation of core-scale experiments using the developed model and commercial software, the saturation tables were first calculated in an excel sheet according to the formulations. The Eclipse data file was then restarted at the beginning of each injection cycle to update the relative permeability data and maintain the saturation distribution in the simulations. This approach is acceptable for core-scale simulations since the system is relatively small, and there is not a significant difference between the saturation histories of the first and last blocks. However, using the developed model in reservoir-scale simulations is not currently possible unless the saturation history of different blocks can be extracted and used for calculating relative permeability data.

During WAG injection at reservoir scale, gas (lighter phase) flows towards the top of the reservoir, while water (heavier phase) sinks to the lower part of the reservoir. Due to this gravitational segregation, a two-phase gas-oil system forms at the top of the reservoir while a two-phase water-oil system exists at the bottom of the reservoir. Three-phase zone exists in the middle of these two-phase regions, and its extent depends on the density difference of fluids present in the reservoir. Therefore, the use of appropriate two- and three-phase hysteresis models is necessary for simulation of each regions considering the unique saturation history of each block.

Figure 21 shows a schematic of different reservoir blocks during an arbitrary second water injection cycle at reservoir-scale (IDI injection scenario). The blocks in the reservoir can have different initial saturations at the beginning of this water injection cycle. The first configuration (a) is expected to be observed in the near-wellbore region, which was first invaded by water

and then by the gas phase. For such saturation history, the relative permeability of the fluids during the second imbibition cycle should be determined using the WAG hysteresis model. The second configuration shows a block that was not invaded during the first water injection cycle but was flooded later during the gas injection cycle. This is likely to happen in the upper blocks of the reservoir when the gravity segregation is active in the system. The first slug of water was not large enough to reach this block, but the second injected was larger and reached this block. This block is undergoing a three-phase flow, but it is at the first imbibition cycle.

Figure 21(c) represents a reservoir block at the bottom of the reservoir, which was already invaded by the water phase during the first water injection. This block was not invaded during the gas injection cycle due to gas override (or because a short gas slug was injected). Hence, this displacement is considered as the second imbibition cycle, and two-phase hysteresis formulations should be used to estimate kr data in this block. Using kr data obtained from a three-phase model for this block can introduce significant errors in the estimation of trapped gas saturation. The last figure, Figure 21(d), shows the schematic of a reservoir block far from the injection well, which has been first invaded during the second water injection cycle. The relative permeability in this block is not affected by the hysteresis phenomenon, and the kr curve for first imbibition cycle should be used.

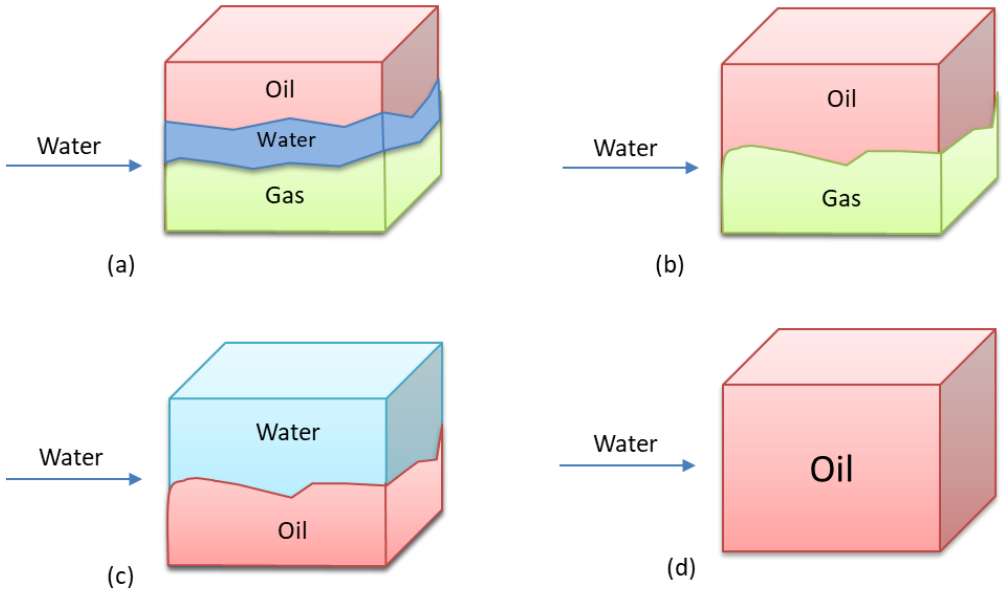


Figure 21: Schematics of reservoir blocks at different initial saturations during the second water injection cycle (IDI injection scenario), (a) second imbibition, three-phase hysteresis (b) first imbibition, three-phase hysteresis, (c) second imbibition, two-phase hysteresis, (d) first imbibition, no hysteresis.

## Summary and Conclusion

In this study, the performance of a new hysteresis model developed at Heriot-Watt University for simulating cyclic multi-phase experiments was evaluated. This new model comprises of several equations for estimation of hysteresis in gas and oil relative permeability, and its parameters are obtained directly from experimental data to eliminate the tuning process. Stone's model was modified to be used in unsteady-state three-phase experiments, and Land's initial-residual relationship was replaced by a new procedure for obtaining final saturations.

The presented model was used for the simulation of six experiments performed on a sandstone sample. The results indicate the model can accurately capture the common trend observed in both two- and three-phase experiments performed at various conditions. The results showed that for WAG experiments performed on sandstones, the final saturations at the end of injection cycles, the total fluid production, and pressure drop curves were estimated successfully. The model was also successfully deployed to capture the cyclic hysteresis observed in two-phase experiments (gas/water, oil/water) performed on a sandstone sample. It was concluded that in cyclic experiments (both two- and three-phase) after a few cycles distinguished flow paths are established for each phase, and less gas is trapped in the system (i.e., the cyclic hysteresis becomes negligible in the system).

## Acknowledgments

This study was conducted in the 'Centre for Enhanced Oil Recovery and CO2 Solutions' at Heriot-Watt University as a part of an ongoing joint industrial project called *Characterization of Three-Phase flow and WAG* is currently equally sponsored by: ADCO, BG Group, Galp Energia, Maersk Oil, Petrobras, Premier Oil, Schlumberger and Total E&P which are gratefully acknowledged. The constructive comments for improving the presented model received from the representatives of these companies at progress meetings are much appreciated.

The authors would also like express their gratitude to Dr. Mobeen Fatemi for performing the core-flood experiments during his PhD studies at HWU. The constructive comments of Prof. Dabir Tehrani as the technical consultant in progress meetings are truly appreciated.

## Nomenclature

$F_g$: Normalized gas relative permeability (Stone's model)

$F_w$: Normalized water relative permeability (Stone's model)

$k_{ro}$ : Oil relative permeability

$k_{rw}$ : Water relative permeability

$k_{rg}$ : Gas relative permeability

$k_{rocw}$ : Oil relative permeability in presence of connate water saturation

$S_o$: Oil saturation

$S_{oi}$: Initial Oil saturation

$S_{of}$: Final Oil saturation

$S_{orw}$: Residual oil saturation after waterflood.

$S_g$: Gas saturation

$S_{gi}$: Initial Gas saturation

$S_{gf}$: Final Gas saturation

$S_w$: Water saturation/ wetting phase saturation

$S_{wf}$: Final water saturation/ Final wetting saturation

$S_{wi}$: Initial water saturation/ Initial wetting saturation

$S_{sim}$: Saturations obtained from simulation

$S_{exp}$: Saturations obtained from experimental data

$SS_o$ : Normalized oil saturation (Stone's model)

$Q_{sim}$: Fluid production obtained from simulation results

$Q_{exp}$: Fluid production obtained from experimental data

**Greek Letters**

$\delta_w$ : Relative difference in water saturation (three-phase) / wetting-phase(two-phase)

$\delta_o$ : Relative difference in oil saturation

$\beta_w$: Reduction in water relative permeability

$\beta_o$ : Reduction in oil relative permeability

$\beta_g$ : Reduction in gas relative permeability

**Abbreviations**

HWU: Heriot-Watt University

WAG: Water Alternating Gas

SSWAG: Short Slug Water Alternative Gas

3P-Kr: Three Phase Relative Permeability

IFT: Interfacial Tension

Exp: Experimental data

Sim: Simulation results

MW: Mixed-Wet sample

WW: Water-Wet sample

NM: Near Miscible condition

ImM: Immiscible condition

I: Imbibition/ Water-injection cycle

D: Drainage/ Gas-injection cycle

OW: Oil/Water

GW: Gas/Water

**References**


1. de Gennes, P.-G., F. Brochard-Wyart, and D. Quere, *Capillarity and Wetting Phenomena: Drops.* Bubbles, Pearls, Waves, 2004: p. 291-291.
2. Juanes, R., et al., *Impact of relative permeability hysteresis on geological CO2 storage.* Water Resources Research, 2006. **42**(12).
3. Beattle, C., T. Boberg, and G. McNab, *Reservoir simulation of cyclic steam stimulation in the Cold Lake oil sands.* SPE (Society of Petroleum Engineers) Reservoir Engineering;(United States), 1991. **6**(2).
4. Skauge, A. and J.A. Larsen. *Three-phase relative permeabilities and trapped gas measurements related to WAG processes*. in *SCA 9421, proceedings of the International Symposium of the Society of Core Analysts, Stavanger, Norway*. 1994.
5. Al-Khdheeawi, E.A., et al., *Enhancement of CO2 trapping efficiency in heterogeneous reservoirs by water-alternating gas injection.* Greenhouse Gases: Science and Technology, 2018. **8**(5): p. 920-931.
6. Larsen, J.A. and A. Skauge, *Methodology for numerical simulation with cycle-dependent relative permeabilities.* SPE Journal, 1998. **3**(02): p. 163-173.
7. Geffen, T.M., et al., *Experimental investigation of factors affecting laboratory relative permeability measurements.* Journal of Petroleum Technology, 1951. **3**(04): p. 99-110.
8. Land, C.S., *Comparison of calculated with experimental imbibition relative permeability.* Society of Petroleum Engineers Journal, 1971. **11**(04): p. 419-425.
9. Carlson, F.M. *Simulation of relative permeability hysteresis to the nonwetting phase*. 1981. Society of Petroleum Engineers.
10. Killough, J.E., *Reservoir simulation with history-dependent saturation functions.* Society of Petroleum Engineers Journal, 1976. **16**(01): p. 37-48.

11. Fatemi, S.M., et al., *Experimental and Theoretical Investigation of Gas/Oil Relative Permeability Hysteresis under Low Oil/Gas Interfacial Tension and Mixed-Wet Conditions.* Energy & Fuels, 2012. **26**(7): p. 4366-4382.
12. Element, D.J., et al. *Assessment of three-phase relative permeability models using laboratory hysteresis data*. 2003. Society of Petroleum Engineers.
13. Duchenne, S., R. de Loubens, and T. Joubert. *Extended three-phase relative permeability formulation and its application to the history-matching of multiple WAG corefloods under mixed-wet conditions*. in *Abu Dhabi International Petroleum Exhibition & Conference*. 2016. Society of Petroleum Engineers.
14. Mahzari, P. and M. Sohrabi, *An improved approach for estimation of flow and hysteresis parameters applicable to WAG experiments.* Fuel, 2017. **197**: p. 359-372.
15. Stone, H.L., *Estimation of three-phase relative permeability and residual oil data.* J. Pet. Technol.;(United States), 1973. **12**(4).
16. Schlumberger, *ECLIPSE Technical Description*. 2018.
17. Aghabozorgi, S., M. Sohtrabi, and J. Facanha. *Estimation of Three-phase Oil Relative Permeability in WAG Experiments*. 2019.
18. Holmgren, C.R. and R.A. Morse, *Effect of free gas saturation on oil recovery by water flooding.* Journal of Petroleum Technology, 1951. **3**(05): p. 135-140.
19. Shahrokhi, O., et al. *Assessment of three phase relative permeability and hysteresis models for simulation of water-alternating-gas (WAG) injection in water-wet and mixed-wet systems*. 2014. Society of Petroleum Engineers.
20. Fatemi, S.M. and M. Sohrabi. *Experimental and Theoretical Investigation of Oil and Gas Trapping Under Two-and Three-Phase Flow Including Water Alternating Gas (WAG) Injection*. 2013. Society of Petroleum Engineers.
21. Shahverdi, H., et al. *Evaluation of three-phase relative permeability models for WAG injection using water-wet and mixed-wet core flood experiments*. in *SPE EUROPEC/EAGE Annual Conference and Exhibition*. 2011. Society of Petroleum Engineers.
22. Aghabozorgi S., S.M., *Detailed Discussion of the Performance of Available Hysteresis Models for Simulation of Cyclic Three-Phase Experiments.* Submitted to Journal of Petroleum Science and Engineering, 2021.
23. Aghabozorgi, S., *Study of multi-phase flow in porous media : modeling of hysteresis and relative permeability data*. 2019, Heriot-Watt University.

24. Shahverdi, H., M. Sohrabi, and M. Jamiolahmady, *A New Algorithm for Estimating Three-Phase Relative Permeability from Unsteady-State Core Experiments.* Transport in Porous Media, 2011. **90**(3): p. 911-926.

25. Sohrabi, M. and S.M. Fatemi, *Experimental Investigation of Oil Recovery by Different Injection Scenarios under Low Oil/Gas IFT and Mixed-Wet Condition: Water-Flood, Gas Injection, WAG and SWAG Injection*. 2012, Society of Petroleum Engineers: Abu Dhabi, UAE. p. 21-21.

26. Alkhazmi, B., M. Sohrabi, and S.A. Farzaneh. *An experimental investigation of the effect of gas and water slug size and injection order on the performance of immiscible WAG injection in a mixed-wet system*. in *SPE Kuwait Oil & Gas Show and Conference*. 2017. Society of Petroleum Engineers.

27. Fatemi, M., et al. *Experimental investigation of oil recovery from carbonate reservoir rocks under oil-wet condition: waterflood, gas injection, SWAG and WAG injections*. in *Abu Dhabi International Petroleum Exhibition and Conference*. 2015. Society of Petroleum Engineers.

28. Fatemi, S.M. and M. Sohrabi, *Cyclic Hysteresis of Three-Phase Relative Permeability Applicable to WAG Injection: Water-Wet and Mixed-Wet Systems under Low Gas/Oil IFT*. 2012, Society of Petroleum Engineers: San Antonio, Texas, USA. p. 21-21.

29. Fatemi, S.M. and M. Sohrabi. *Experimental and numerical investigation of the impact of design parameters on the performance of WAG and SWAG injection in water-wet and mixed-wet systems*. in *SPE Enhanced Oil Recovery Conference*. 2013. Society of Petroleum Engineers.

30. Alkhazmi, B., et al. *A Comprehensive and Comparative Experimental Study of the Effect of Wettability on the Performance of Near Miscible WAG Injection in Sandstone Rock*. in *SPE Annual Technical Conference and Exhibition*. 2018. Society of Petroleum Engineers.

31. Fatemi, M. and M. Sohrabi, *Mechanistic study of enhanced oil recovery by gas, WAG and SWAG injections in mixed-wet rocks: Effect of gas/oil IFT.* Experimental Thermal and Fluid Science, 2018. **98**: p. 454-471.

32. Fatemi, S.M. and M. Sohrabi. *Mechanistic study of the effect of gas/oil IFT on the performance of gas, WAG and SWAG injections in mixed-wet systems*. in *SPE Annual Technical Conference and Exhibition*. 2015. Society of Petroleum Engineers.

33. Alkhazmi, B., et al. *An Experimental Investigation of WAG Injection Performance under Near-Miscible Conditions in Carbonate Rock and Comparison with Sandstone*. in *SPE Western Regional Meeting*. 2018. Society of Petroleum Engineers.

34. Fatemi, M. and M. Sohrabi, *Multiphase flow and hysteresis phenomena in oil recovery by water alternating gas (WAG) injection*. 2015, Heriot-Watt University.

35. Hustad, O.S. and T. Holt. *Gravity stable displacement of oil by hydrocarbon gas after waterflooding*. 1992. Society of Petroleum Engineers.

36. Aghabozorgi, S. and M. Sohrabi, *A comparative study of predictive models for imbibition relative permeability and trapped non-wetting phase saturation.* Journal of Natural Gas Science and Engineering, 2018. **52**: p. 325-333.